

A LAST LOOK AT THE MICROWAVE HAZE/BUBBLES WITH WMAP

GREGORY DOBLER^{1,2}*Draft version November 8, 2018*

ABSTRACT

The microwave “haze” was first discovered with the initial release of the full sky data from the Wilkinson Microwave Anisotropy Probe. It is diffuse emission towards the center of our Galaxy with spectral behavior that makes it difficult to categorize as any of the previously known emission mechanisms at those wavelengths. With now seven years of WMAP data publicly available, we have learned much about the nature of the haze, and with the release of data from the *Fermi Gamma-Ray Space Telescope* and the discovery of the gamma-ray haze/bubbles, we have had a spectacular confirmation of its existence at other wavelengths. As the WMAP mission winds down and the *Planck* mission prepares to release data, I take a last look at what WMAP has to tell us about the origin of this unique Galactic feature. Much like the gamma-rays, the microwave haze/bubbles is elongated in latitude with respect to longitude by a factor of roughly two, and at high latitudes, the microwave emission cuts off sharply above ~ 35 degrees (compared to ~ 50 degrees in the gammas). The hard spectrum of electrons required to generate the microwave synchrotron is consistent with that required to generate the gamma-ray emission via inverse Compton scattering, though it is likely that these signals result from distinct regions of the spectrum (~ 10 GeV for the microwaves, ~ 1 TeV for the gammas). While there is no evidence for significant haze polarization in the 7-year WMAP data, I demonstrate explicitly that it is unlikely such a signal would be detectable above the noise.

Subject headings: Galaxy: center — ISM: structure — ISM: bubbles — Radio continuum: ISM

1. INTRODUCTION

With the initial release of the full sky data by the *Wilkinson Microwave Anisotropy Probe* (WMAP, Bennett et al. 2003b) came the discovery that there was anomalously hard spectrum microwave emission towards the center of our Galaxy (Finkbeiner 2004a). The method for uncovering this WMAP “haze” as it was termed at the time was very simple: there were known or anticipated microwave emission mechanisms from the Galaxy and it was believed that templates (maps at other wavelengths) morphologically tracing these foregrounds could be used to clean Galactic emission from the maps for CMB analysis and to study the foregrounds in their own right (Bennett et al. 2003a) using straightforward linear regression techniques. These templates were known to be insufficient down to the measurement noise in the WMAP maps, yet the template fitting procedures worked remarkably well for both the cosmological (Spergel et al. 2003) and Galactic science purposes.

However, while removing $>95\%$ of the variance in the data (Finkbeiner 2004a; Dobler & Finkbeiner 2008a) the templates failed most spectacularly within $\sim 30^\circ$ of the Galactic center (GC). After removing the emission correlated with the templates, the residual resembled a “hazy” blob with a spectrum that was too soft to be free-free emission and too hard to be synchrotron emission from electrons generated by supernova (SN) remnants (Dobler & Finkbeiner 2008a, hereafter DF08). This microwave haze is somewhat elongated in Galactic latitude with an intensity falling off with distance from the GC. A careful measurement of the spectrum and radial dependence of the haze by DF08 led to ample speculation

about the origin of the haze electrons: from star formation and SN acceleration (Biermann et al. 2010) to signatures of particle dark matter annihilation in our Galactic halo (Hooper et al. 2007; Cholis et al. 2009a,b) to claims that the feature did not exist at all (Mertsch & Sarkar 2010).

The last of these claims was laid to rest with the first year data release of the *Fermi Gamma-Ray Space Telescope* which showed a similar structure at gamma-ray energies Dobler et al. (2010). The implication was that the same electrons that generate microwaves at WMAP wavelengths generate gammas via inverse Compton (IC) scattering that are observed by *Fermi*. It was also found by Dobler et al. (2010) that, while the extent of the microwaves is $\sim \pm 30^\circ$, the gamma-ray haze extended to a full $\pm 50^\circ$ above and below the Galactic plane, making it the second largest structure in our Galaxy after the Galactic disk (assuming that it is centered roughly on the GC) with a top-to-bottom length of 20 kpc. Furthermore, analysis of 1.6 years of *Fermi* data by Su et al. (2010) suggests that the gamma-ray emission also has sharp edges and it was renamed the “bubbles”. Given the established correspondence between the WMAP “haze” and the *Fermi* “haze/bubbles”, I will refer to the microwave emission as the WMAP “haze/bubbles” or “haze” interchangeably throughout this paper.³

We now have the benefit of six additional years of microwave data from WMAP and clues from the *Fermi* gammas. Given that the release of the *Planck* data is

¹ Kavli Institute for Theoretical Physics, University of California, Santa Barbara Kohn Hall, Santa Barbara, CA 93106 USA

² dobler@kitp.ucsb.edu

³ Historically, there has been some ambiguity to the nomenclature and to what the term “haze” refers. Given the observations, the clearest definition would be that the haze is a population of anomalously hard spectrum cosmic-rays towards the GC and the microwave and gamma-ray haze/bubbles are observed signals generated by those cosmic-rays.

scheduled for late 2012, I will present a description of what we know about the haze/bubbles at the end of the WMAP era and the beginning of the *Planck* era. In particular, in §2 I will describe the methods used to uncover the haze in the first place and comment on other component separation techniques. In §3 I present the 7-year WMAP haze/bubbles spectrum and morphology and describe new findings at high latitude. In §4 I address the state of the haze in the WMAP polarization data and in §5 I discuss the merits and demerits of the various proposals for the origin of the haze/bubbles electrons before summarizing in §6.

2. COMPONENT SEPARATION

Component separation in the context of CMB foregrounds is a broad term for identifying and removing (separating) Galactic emission mechanisms from the data. Template fitting is perhaps the most basic of the available techniques but has proven to be *remarkably* powerful despite its simplicity. The fundamental equation to be solved is just a linear fit of templates to the data: $\mathbf{w} = \mathbf{P}\vec{a}$ where \mathbf{w} is a map of the WMAP data, \mathbf{P} is a matrix of template maps, and \vec{a} is a vector of amplitudes. The least-squares solution to this equation (after taking the noise map \mathbf{n} into account) is $\vec{a} = (\mathbf{P}^T \mathbf{n}^{-1} \mathbf{P})^{-1} (\mathbf{P}^T \mathbf{n}^{-1} \mathbf{w})$. This formalism easily accommodates partial sky coverage and arbitrary numbers of templates. Of course, for the purpose of studying Galactic foregrounds, one of the templates must be a CMB estimate with an input CMB spectrum, and as shown in DF08 (as well as Dobler & Finkbeiner 2008b; Dobler et al. 2009), this introduces a bias in the derived foreground spectra because no CMB estimate is ever completely clean of the very foregrounds to be measured.

When applying template fitting to the WMAP 7-year temperature data using the templates and partial sky regions defined in DF08 (to take into account foreground spectral variation with position), the 7-year WMAP haze/bubbles emission is shown in Figure 1. However, I have made two adjustments to the templates used in the fit compared to DF08. First, for the haze template, I use a bivariate Gaussian of scale length $\sigma_\ell = 15^\circ$ and $\sigma_b = 25^\circ$. Second, the haze residual in DF08 included a significant “disky” component near the mask likely associated with energy dependent propagation lengths of electrons accelerated in the Galactic disk as discussed in Mertsch & Sarkar (2010). This is a failing of using the Haslam 408 MHz map (Haslam et al. 1982) as a soft synchrotron template. Additionally, there is the possibility that a population of pulsars in the Galactic disk could potentially produce harder spectrum cosmic-ray electrons.⁴ Whatever its origin, this disky component likely does not represent true haze emission and as such I include a Gaussian disk template with scale lengths $\sigma_\ell = 20^\circ$ and $\sigma_b = 5^\circ$. The mask used to fit the data excludes regions where the dust extinction at $H\alpha$ is greater than 1 magnitude as well as all point sources in both the WMAP and *Planck* ERCSC (30 GHz to 143 GHz) catalogs, the LMC, SMC, M31, Orion-Barnard’s Loop, NGC

5128, and ζ -Oph.

As seen in Figure 1, outside of the haze region, the residuals are remarkably small, indicating that the templates used in the analysis do represent reasonable tracers of the actual emission.⁵ Most importantly, several authors have found that emission from rapidly rotating dust grains (which have small dipole moments and thus produce spinning dipole radiation) represents $>30\%$ of the diffuse emission at K-band (see DF08 and Finkbeiner 2004a). This spinning dust is perhaps the most uncertain foreground since it is not well known how its emissivity scales with total dust column density (inferred from $100\mu\text{m}$ for example).

In addition to the simple template fitting described above, more involved component separation techniques have been developed and applied to the WMAP data. The two most commonly used are the Maximum Entropy Method (Bennett et al. 2003a) and Bayesian inference via Gibbs sampling (Eriksen et al. 2006). While these methods are excellent for cleaning the CMB of foregrounds and estimating the amplitude of emission with known morphology (such as the cosmic dipole), they are not optimal for identifying new components. For example, although it has been reported that these techniques do not “see” the WMAP haze/bubbles, in fact Pietrobon et al. (2011) show that the haze emission is typically swept into a “low frequency” component that is a conglomerate of spinning dust, soft synchrotron, hard synchrotron, and free-free all forced to obey a single power law spectrum.

3. SPECTRUM AND MORPHOLOGY

3.1. The Haze at Low Latitudes

The residuals in Figure 1 and the spectrum plots in Figure 2 show the two important features of the microwave haze/bubbles. First, the spectrum is very hard, $T_H \propto \nu^{\beta_H}$ with $\beta_H \approx -2.5$ which is harder than can be obtained from particle acceleration in SN shocks after taking into account cosmic-ray diffusion and energy losses. However, it is significantly *softer* than the $\beta_F = -2.15$ required if the emission were free-free. Second, the haze/bubbles are extended and elongated in latitude. In detail however, while the haze is roughly centered on the GC, its morphology is somewhat different in the north and south. In the south, and above latitude $b = -30^\circ$, the morphology of the WMAP haze/bubbles is strikingly similar to the *Fermi* haze/bubbles (right panel of Figure 1). In the north, the situation is much more complicated by the significant dusty regions of the Ophiuchus complex. In fact, the direction of the north Galactic center (below $b = 30^\circ$) likely contains either significant spinning dust emission that is not well approximated by our dust template (the Schlegel et al. (1998) dust map evaluated at 94 GHz by Finkbeiner et al. (1999)) or highly variable gas temperatures making our free-free template

⁴ However, the efficiency factor for generating electrons with pulsars is presently not constrained (and could be as low as zero), while Mertsch & Sarkar (2010) showed that the energy dependent propagation effects are of roughly the right order of magnitude given the results in §3.

⁵ The one exception is the Gum Nebula at $\ell \sim -100^\circ$; there are two reasons for this. First, as pointed out in DF08 and Dobler et al. (2009), the gas temperatures and spinning dust spectra are varying very rapidly with position in this region. Second, the Gum Nebula is one of the brightest Galactic regions in the raw data and so these residuals actually represent a small fraction of the total emission. Also, it is important to note that the Gum Nebula is relatively nearby and as such occupies a *much* smaller volume than the haze/bubbles.

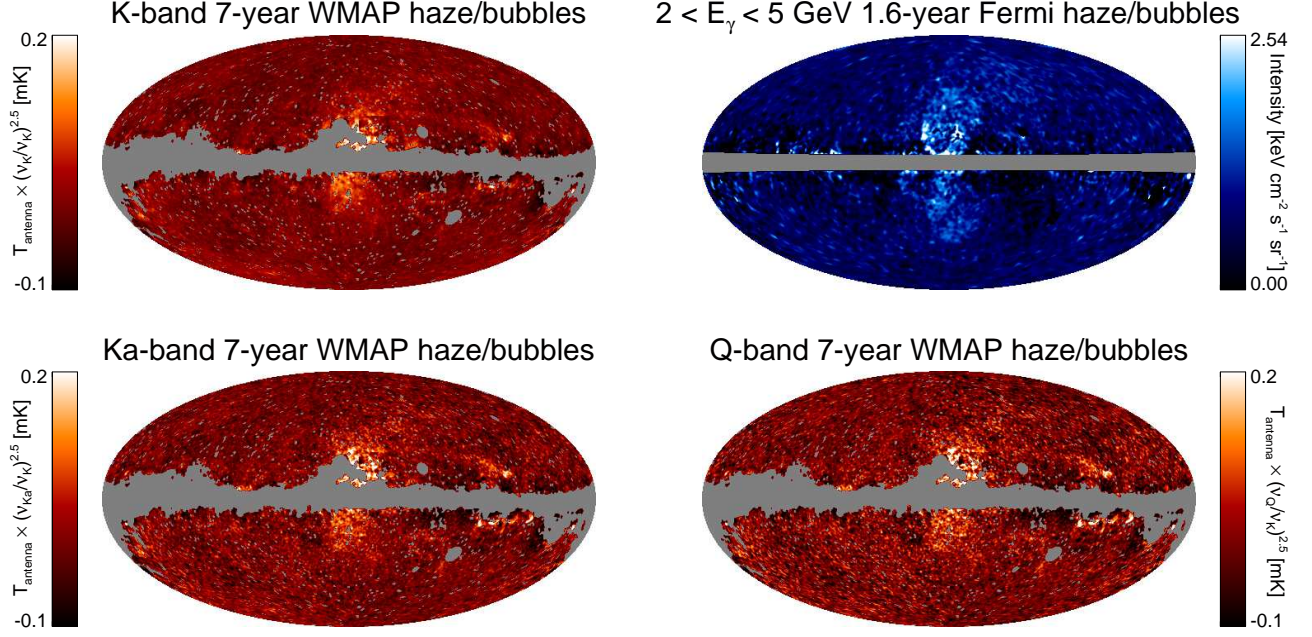


FIG. 1.— The haze/bubbles in both microwaves and gamma-rays (23 GHz, 33 GHz, 41 GHz, and 2-5 GeV, counter clockwise from top left). In the microwaves, templates have been used to regress out emission from the CMB, thermal and spinning dust, free-free, and soft synchrotron. In the gammas, the official *Fermi* diffuse model has been subtracted from the data (see Dobler et al. 2010). In all bands, the haze is seen to be elongated in latitude by a factor of roughly two reaching $\pm 50^\circ$ in the gammas and $\sim \pm 35^\circ$ in the microwaves. The microwaves are stretched with a $\nu^{2.5}$ scaling, which yields roughly equal brightness from K to Q band, indicating an electron spectrum of $dN/dE_e \propto E_e^{-2}$, broadly consistent with the gamma-ray spectrum from Dobler et al. (2010) and Su et al. (2010). The gamma-ray haze/bubbles seem to have a sharp edge near $|b| \sim 50^\circ$ while the microwaves seem to fall off quickly for $|b| > 30^\circ$ (particularly in the south).

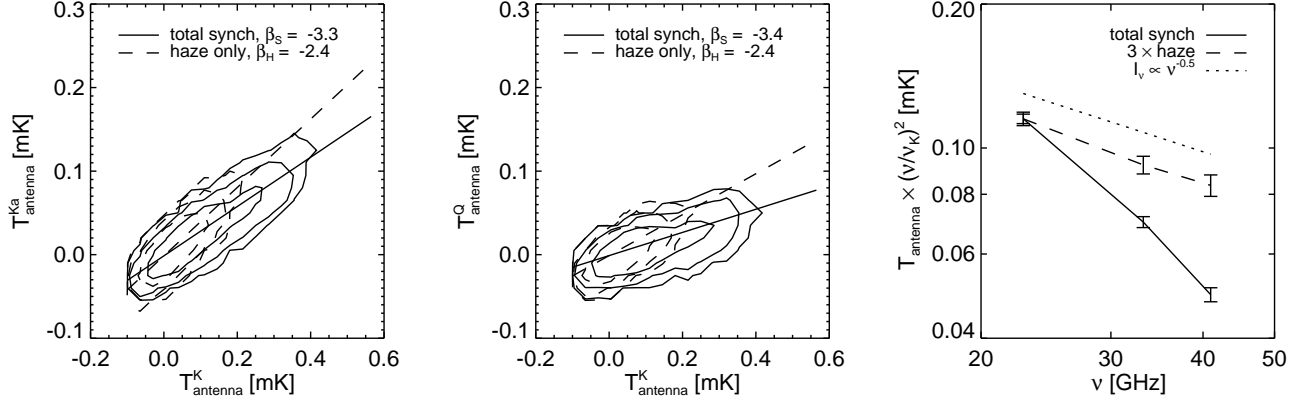


FIG. 2.— *Left and middle*: scatter plots (drawn with contours) for the microwave haze/bubbles residuals in Figure 1 (dashed lines) and for the total synchrotron (haze plus soft synchrotron; solid lines) in the region $|l| < 25^\circ$, $-35^\circ < b < -10^\circ$. The best fit power law for this region shows that the haze emission is significantly *harder* than the soft synchrotron from 23 GHz to 41 GHz. The total emission in the region for both cases is shown in the *right* panel. The haze emission is clearly harder given the noise in the data, is consistent with a power law of roughly $\nu^{-2.5}$, and represents approximately 33% of the total synchrotron emission at K-band.

(the Finkbeiner (2003) $H\alpha$ map) unreliable. In reality, both effects are likely operating simultaneously.

This additional complexity in the north is the reason that I concentrate on the south when estimating the spectrum of the haze in Figure 2. The derived spectrum of $\beta_H \approx -2.5$ implies an electron spectrum of $dN/dE_e \propto E_e^{-2}$ which has been shown by Dobler et al. (2010) and Su et al. (2010) to be broadly consistent with the spectrum of the *Fermi* gamma-ray haze/bubbles. This, taken together with the morphological correlation at low latitudes, provides the strongest evidence that this is in fact the same phenomenon observed at multiple wavelengths. While it is true that DF08 showed

that the bias induced by presubtracting a CMB estimate can be quite large, for a component with a spectrum $T \propto \nu^{-2.5}$ the CMB5 weights for the WMAP7 data ($\zeta = [0.246, -0.736, -0.0685, 0.263, 1.295]$ in thermodynamic ΔT for the five WMAP bands) would lead to a measured spectrum $\propto \nu^{-2.53}$ when comparing K- to Ka-band and $\propto \nu^{-2.54}$ when comparing K- to Q-band. In other words, the bias for a foreground with a haze/bubbles-like spectrum would be rather small given the DF08 CMB5 estimate and so $\beta_H = -2.5$ is likely *very* close to the true spectrum. Furthermore, a component with a free-free spectrum would be inferred to have a spectrum of $\propto \nu^{-2.154}$ providing more evidence that the

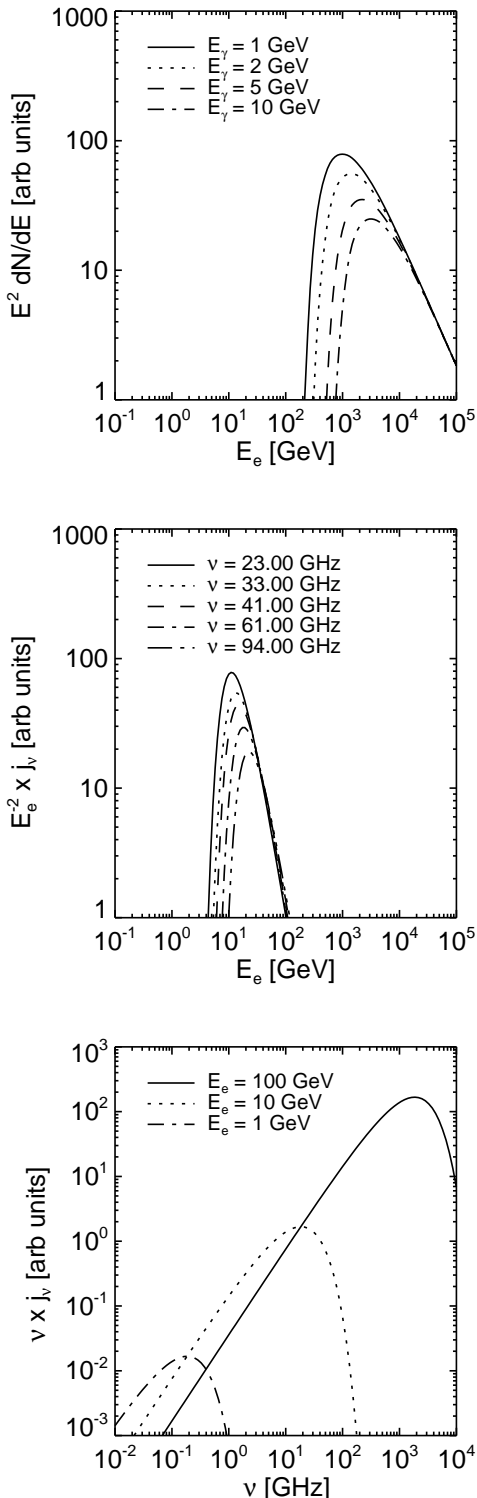


FIG. 3.— *Top and middle*: intensity in CMB IC scattered gammas and microwave synchrotron as a function of the electron energy for a population of electrons with spectrum $dN/dE_e \propto E^{-2}$ illustrating that the WMAP haze/bubbles and *Fermi* haze/bubbles are generated by different ranges of the electron spectrum. In particular, if the gammas at ± 10 kpc are generated by scattering of CMB photons, this requires \sim TeV electrons at those distances, while the microwaves are generated by electrons with energies ~ 10 GeV. The higher energy electrons used to generate the gammas would create a synchrotron signal that peaks at very high frequencies (*bottom*), though it would be overshadowed by thermal dust emission.

microwave haze/bubbles is *not* due to free-free emission.

However, it is important to bear in mind that the majority of the haze/bubble gammas observed by *Fermi* at high latitudes likely come from $E_e > 100$ GeV electrons scattering CMB photons, while the microwaves are generated by electrons with energies $1 \text{ GeV} < E_e < 100 \text{ GeV}$. This is illustrated in Figure 3 which shows the total emissivity

$$j_\nu^{\text{tot}} = \int E_e j_\nu(E_e, B) \frac{dN}{dE_e} d \ln E_e, \quad (1)$$

where j_ν is the emissivity from a single electron at energy E_e in a magnetic field B , as a function of electron energy for a population of electrons with the haze/bubbles spectrum in a $5 \mu\text{G}$ magnetic field. It is also worthwhile to note that, as shown in the figure, if the electron energy extends up to order TeV energies as required by the gammas, then the synchrotron emissivity per electron for $E_e > 100$ GeV actually increases with increasing frequency. However, the falling electron spectrum and emission from thermal dust (which rises much faster with frequency) render this high frequency synchrotron undetectable.

3.2. The Haze at High Latitudes

An aspect of the haze/bubbles that has not been fully discussed is the behavior of the microwave emission at *high* latitudes, where the gamma-ray signal is most unambiguous and where the microwaves appear to fall off in intensity. Figure 4 shows the microwave and gamma-ray haze side-by-side, with a large $\pm 28^\circ$ mask and smoothed to a common 2° beam. It is immediately clear from the figure that there most certainly *is* haze emission above $|b| = 28^\circ$, but its morphology is somewhat different than the gammas.

Concentrating again mostly on the south, the gammas fill a bubble with a sharp edge while the microwaves seem to fall off dramatically for $b < -35^\circ$ as shown in the lower left panel of Figure 4. The intensity as a function of latitude within the bubble (defined by the gamma-ray emission), does not quite have an “edge” in the same sense as the gammas, but the fall off is quite rapid indicating either a rapid decrease in the number of electrons or the strength of the magnetic field. Given the gammas at latitudes $-50^\circ < b < -35^\circ$, the latter seems more likely. Furthermore, given that neither synchrotron maps at lower frequencies (e.g., the 408 MHz map) nor WMAP polarization show a sharp drop in synchrotron emission below $b = -35^\circ$, this seems to indicate that the dominant field component producing the synchrotron is the field within the haze/bubbles itself rather than the Galactic magnetic field. Assuming that the haze/bubbles is located at the GC, then the scale height of this magnetic field drop off is ~ 6 kpc.

The “sharpness” of the microwave edge is depicted in Figure 5 which shows the total intensity as a function of both latitude and longitude in the south. Interestingly, for latitudes $-35^\circ < b < -6^\circ$, the brightness is roughly flat with distance. There is some slow decrease, but the drop below $b = -35^\circ$ is striking, and this flatness is reminiscent of the gamma-ray emission — though again, the edge is not as sharp and is at lower absolute latitude. This latitudinal profile is qualitatively different from that presented in DF08 in which the haze brightness increases

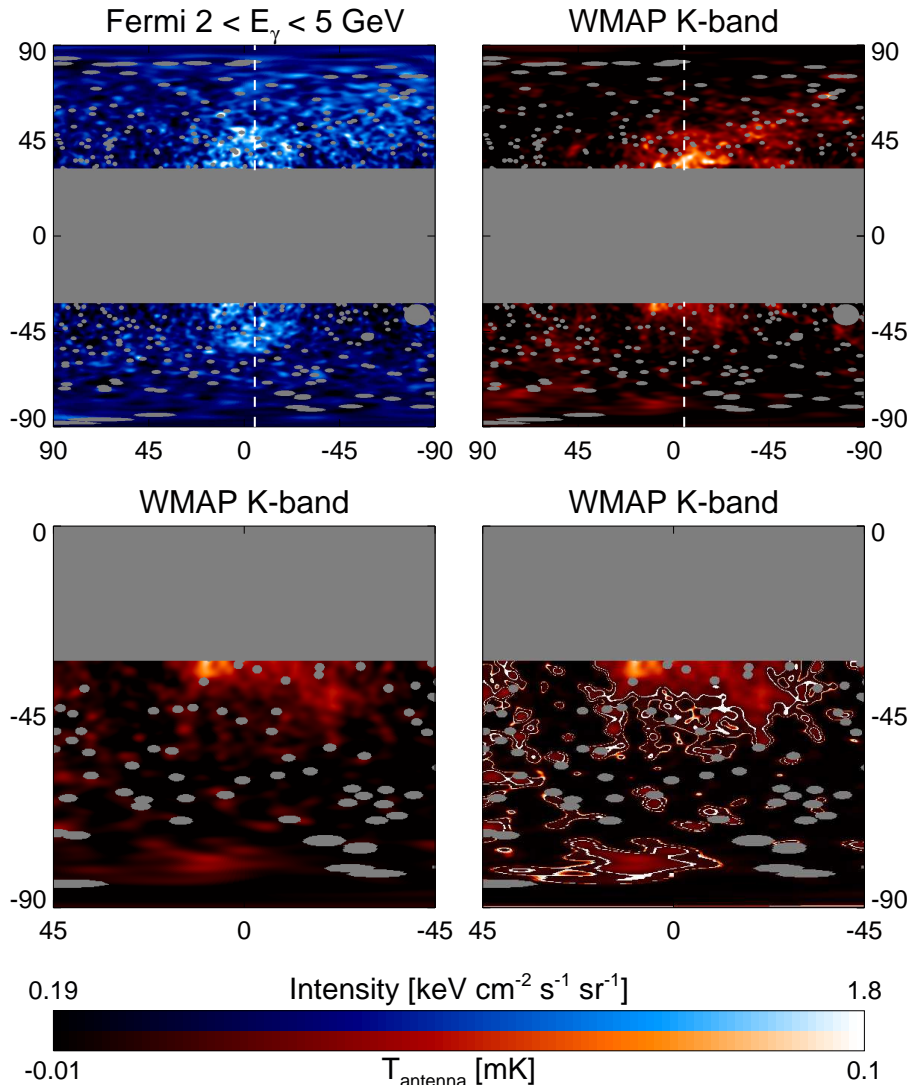


FIG. 4.— The *Fermi* (top left) and WMAP (top right) haze/bubbles at high latitudes masking emission for $|b| < 28^\circ$. The correlation between the two is clear, though the microwave “edge” is at a lower latitude than the gamma-ray edge, indicating that the “bubble” is not completely filled by microwaves. The dashed white line at $\ell = -5^\circ$ illustrates that, while the haze/bubbles is centered on the GC at low latitudes, it is offset by a few degrees above $|b| \sim 28^\circ$. The sharp drop in microwaves in the Galactic south (bottom left) indicates either a sharp decrease in the total number of electrons or a sharp drop in the magnetic field. The former seems unlikely given the presence of gammas down to $b \sim -50^\circ$. Bottom right the same stretch, but with contours showing $T_{\text{antenna}} = 10^{-2}$ and 10^{-3} mK indicating the very sharp transition from haze/bubbles to noise below $b \sim -30^\circ$ (see also Figure 5).

sharply towards the GC above $b = -10^\circ$. The difference is that the inclusion of the extra disk template (to account for the excess disk emission near the mask) has removed most of this power making the profile “flatter” with latitude. As a function of longitude, again the haze brightness is roughly constant within about $|\ell| < 15^\circ$ outside of which the fall off is quite rapid. The figure also shows that for latitudes $-50^\circ < \ell < -40^\circ$, there is *no* significant microwave haze/bubbles emission, in contrast to the gammas.

In the north, again the situation is somewhat complicated since there is clearly emission co-located in both the microwaves and gammas, but there is also significant contamination by spinning dust in the microwaves and π^0 decay photons in the gammas. Nevertheless, it is clear from the morphology (see Figure 4) that, while the lower latitude microwaves are centered on the GC, the center of the structure at $|b| = 28^\circ$ is roughly $\ell = -5^\circ$, an offset

which causes some difficulty for formation scenarios.

4. POLARIZATION

Given the spectrum derived in Figure 2, the haze emission certainly seems to be consistent with hard spectrum synchrotron. Also given that synchrotron with $\beta \approx -2.5$ can be up to 70% polarized in a completely ordered magnetic field, this raises the question whether the haze appears in WMAP polarization data. Several authors have addressed this issue, most notably Gold et al. (2011) who claim no evidence for a significant hard component from WMAP 7-year data. However, this claim suffers from two major drawbacks. First, as shown in Miville-Deschênes et al. (2008) and argued in DF08, even a small turbulent component in the magnetic field can reduce the polarization amplitude when projecting along the line of sight. In fact, this line of sight depolarization is clearly observed in the WMAP data as illustrated

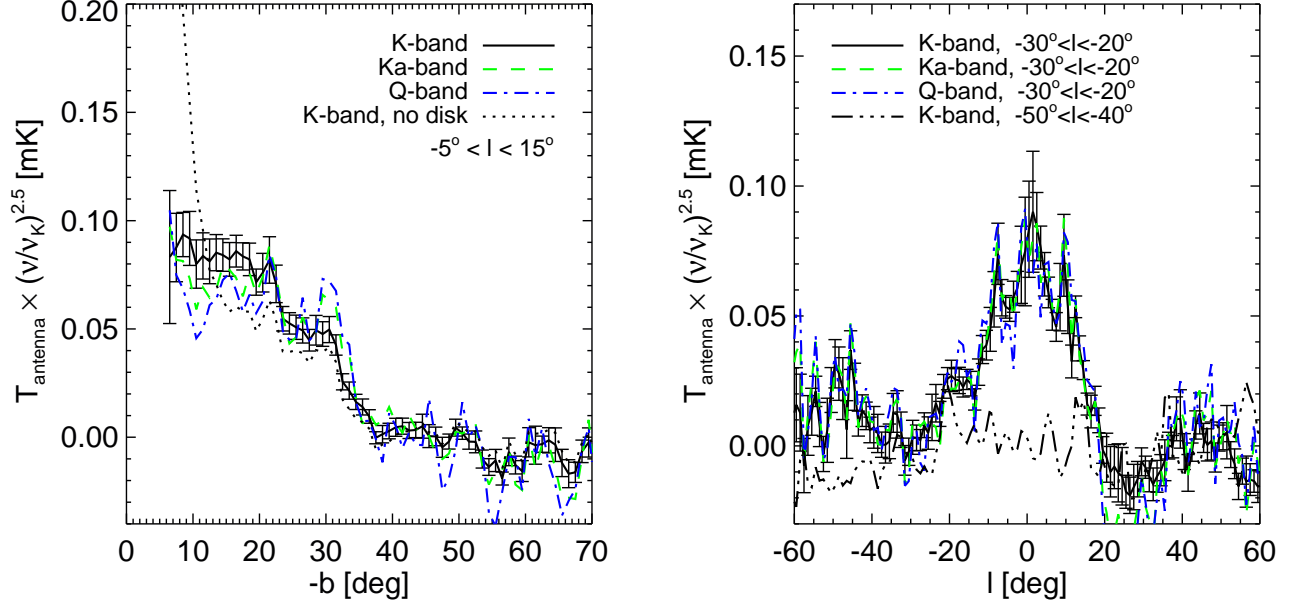


FIG. 5.— The microwave haze/bubbles profile as a function of latitude (*left*) and longitude (*right*). Inside of the haze region, the brightness is roughly flat (or at most, decreases slowly with latitude) and then drops sharply for latitudes below $b \approx -35^\circ$ and for longitudes $|l| > 15^\circ$. This “edge” in the microwaves is not as sharp as in the gammas, and the dotted line in the right panel indicates that there is little to no microwave emission for latitudes $-50^\circ < b < -40^\circ$, in contrast with the gamma-ray measurements, indicating a relatively quick drop in the magnetic field at $b \sim -35^\circ$. The dotted line in the left panel shows the results without including the bivariate Gaussian disk template. In that case, the profile rises dramatically towards the GC, but this emission is not likely to be associated with the haze (see §2).

in Figure 6 which shows that (outside of the mask used in the fits), almost *all* of the emission is due to Loop I which is a local feature. The disk synchrotron is simply not present in the polarization data though it is seen in the total intensity data, indicating that most of the disk emission is line-of-sight depolarized by the varying orientation of the Galactic magnetic field.

As Figure 6 illustrates, the second shortcoming is that, even if the polarization fraction of the haze were constant with respect to the polarization fraction of prominent features like the Loop I SN remnant, the noise in the polarization data is prohibitively large to detect a harder synchrotron component. The argument goes as follows, forming the polarization residual

$$R_P = P_{\text{Ka}} - P_K \times \left(\frac{\nu_{\text{Ka}}}{\nu_K} \right)^{-3.3}, \quad (2)$$

where P_i and ν_i are the WMAP polarization map and frequency at band i respectively, produces a map consistent with noise as shown in Figure 6. That is, all of the emission (synchrotron in the case of polarization) outside of the mask is consistent with having a single power law spectrum $\beta_S = -3.3$. However, if we make the same residual using just the synchrotron intensity S_i ,

$$R_I = S_{\text{Ka}} - S_K \times \left(\frac{\nu_{\text{Ka}}}{\nu_K} \right)^{-3.3}, \quad (3)$$

where S_i is the template extracted synchrotron (i.e., the raw data minus the CMB, thermal plus spinning dust, and free-free components), Figure 6 shows that this residual *also* shows no evidence of the haze. However, we *know* that the haze is there and that its spectrum is harder than elsewhere in the Galaxy from Figures 1-4 and Figure 7 of DF08. The conclusion is that, given the

short lever arm of 23-33 GHz, even the temperature data are too noisy to extract a slightly harder spectrum component in this manner, let alone the polarization data.

5. ORIGIN SCENARIOS

Since the haze/bubbles was first discovered in the microwaves by Finkbeiner (2004a), and especially since the recent discovery in the gammas by Dobler et al. (2010), there has been significant effort devoted to theorizing about the origin of this hard spectrum population of electrons. Each scenario has associated pros and cons, successfully producing some aspects of the emission and failing to produce others. The following is a list of the leading possibilities put forth in the literature.

Galactic wind: The Galactic wind scenario (Crocker et al. 2011; Crocker & Aharonian 2011) suggests that cosmic-rays are accelerated to $\sim \text{TeV}$ energies, that the gammas are the result of collisions of cosmic-ray protons with a very underdense ISM in the bubbles producing π^0 decay emission, and that the microwaves represent the synchrotron from secondary electrons. This model can reproduce the hard spectrum WMAP signal and, because the proton spectrum is also very hard, the hard spectrum gamma-rays as well. The primary failing of this model is that it requires extended injection of cosmic-rays over several billions of years, making the sharp edge of the gammas and microwaves very difficult to maintain over those long time scales. Additionally, even in the event where the ISM is “saturated” with protons as they describe, the bubbles will produce constant volume emissivity leading to limb darkening of the gammas contrary to observations. Finally, as in observed winds in other galaxies (Veilleux et al. 2005), we would expect to see a significant cool component producing $\text{H}\alpha$ emission, but no $\text{H}\alpha$ associated with the haze/bubbles

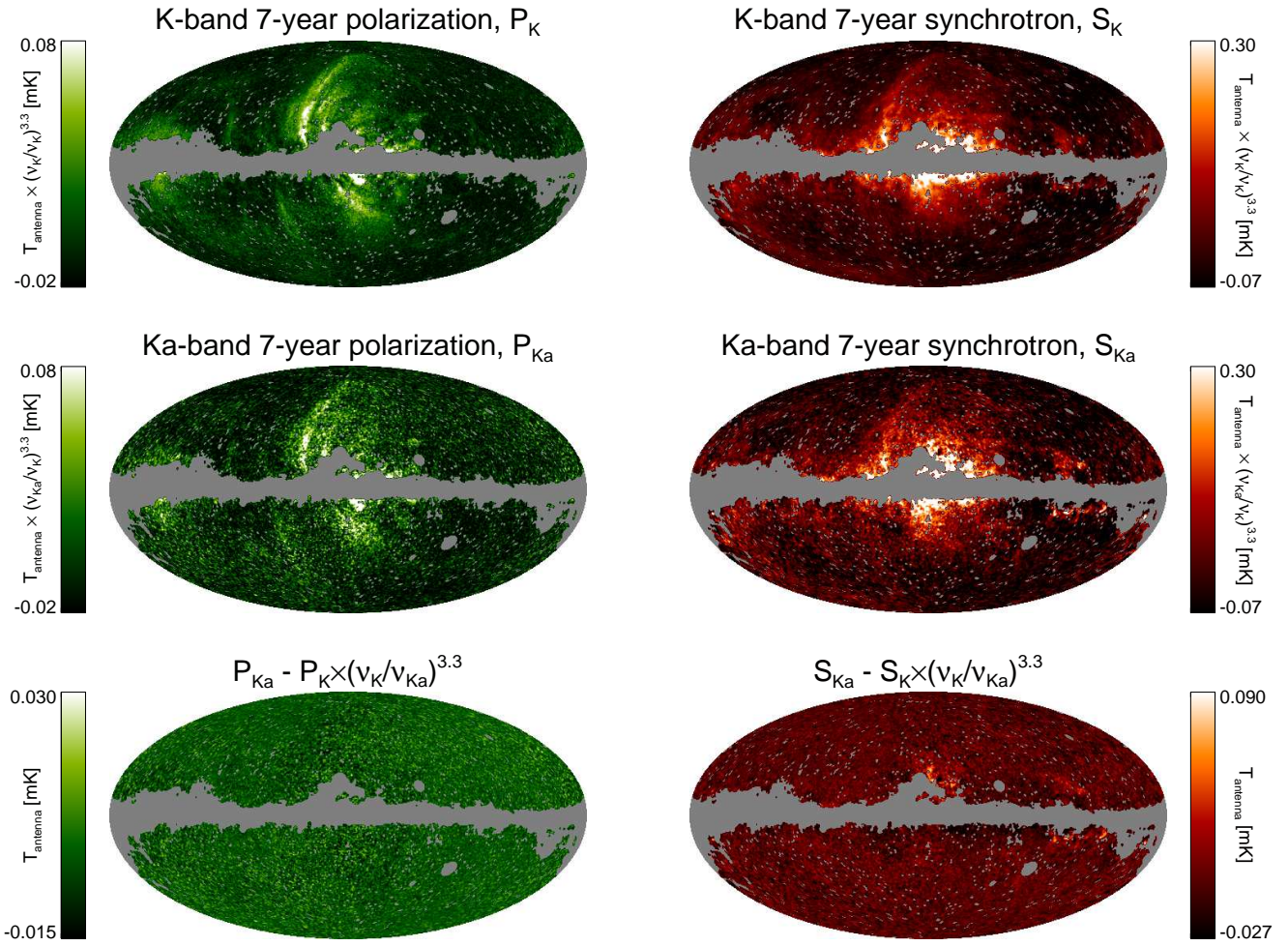


FIG. 6.— The WMAP polarization (*left*) and total synchrotron intensity (*right*) at K- and Ka-band (*top two rows*). Although some features are similar (namely Loop I in the North), there are significant regions of synchrotron intensity that do not appear in polarization (e.g., the Galactic plane) indicating line-of-sight projection effects through a turbulent magnetic field that reduce the total polarized signal. Scaling P_K by a single $\beta = -3.3$ power law across the whole sky and then subtracting from P_{Ka} yields residuals consistent with noise (*bottom left panel*) potentially indicating that the haze does not appear in polarization. However, a similar exercise with the total intensity also yields similar results (*bottom right panel*) *despite* the fact that the haze/bubbles are there and have a different spectrum (see Figures 1 and 2). The implication is that the 23-33 GHz lever arm is too small and the noise in the polarization data too large to positively identify or rule out a polarized haze/bubbles component.

has yet been observed (DF08; Su et al. 2010).

Starburst/SNe: In this scenario a significant outflow is generated by star formation and/or SNe in the GC (e.g., Biermann et al. 2010). However, this model would not only likely lead to associated $H\alpha$, but it is not clear how the uniform intensity gammas are produced or the sharp edges. Furthermore, the timescale for the cosmic-rays to reach 5-10 kpc as required by the microwave and gamma-ray data implies that the spectrum would be rendered too soft to reproduce the haze/bubbles given that the energy loss time for ~ 100 GeV electrons is $\tau \sim 10^5 - 10^6$ yr. Reacceleration of the cosmic-rays is a possibility, but what the reacceleration mechanism is above a few kpc is unclear.

Second order Fermi acceleration: Rather than an actual “formation” mechanism, this model relies on the haze/bubbles to be generated by, for example, a GC jet (see below) which is then filled with magnetosonic turbulent waves that accelerate particles (Mertsch & Sarkar 2011). At the source of injection, the electron spectrum is $dN/dE_e \propto E_e^{-2}$. This scenario suffers from having relatively little predictive power since the absolute num-

ber of accelerated electrons relies on the microphysics of the acceleration mechanism (which is not well known) and the injection morphology can be set somewhat arbitrarily (though it must be concentrated near the outer shock). Furthermore, as found by Mertsch & Sarkar (2011), for the required parameters to explain the gammas, the WMAP haze is underpredicted by an order of magnitude. This tension can be alleviated somewhat by increasing the magnetic field strength, but this would predict microwaves below $b = -35^\circ$ (and indeed a bubble edge in the microwaves at $|b| \sim 50^\circ$) which is not seen in the data.

Active Galactic nucleus: One of the most promising scenarios is that there was some accretion event onto the central Galactic black hole roughly 1 million years ago that resulted in a GC jet (Guo & Mathews 2011). This model is attractive mainly because it is episodic (meaning that it can more easily explain the sharp edges in the gammas) and it can produce roughly the required integrated power in gammas and microwaves. There are four primary concerns with the model however. First, as shown by Su et al. (2010) the intensity profile of the

gammas is roughly uniform and, at best, the AGN model would predict a uniform volume emissivity, again yielding limb darkening, especially near the base of the jet generated bubble which is very thin. Second, generically, shearing instabilities are generated at the edge which are not seen in the gamma ray data which has smooth edges. However, viscosity within the plasma can effectively suppress the instabilities (Guo et al. 2011). Additionally, magnetic draping may suppress the instabilities (and have the added benefit of confining the cosmic-rays as required), though it has not yet been shown that the required field strengths would not produce synchrotron at latitudes $|b| > 35^\circ$ which is not observed. Relatedly, the third concern is that, from jets in other galaxies, we see radio lobes – large bubbles of radio emission at high latitudes (e.g., Schreier et al. 1979). As shown in Figure 1 however, the WMAP haze is confined to lower latitudes and large radio lobes coincident with the gamma-rays are not present. Finally, while the integrated power is sufficient to explain the haze, the model has the significant disadvantage that it has yet to predict a spectrum for the accelerated electrons, which is a key characteristic of the haze. The softening argument from above still applies here and the requirements are that the spectrum 10 kpc away from the event have $dN/dE_e \propto E_e^{-2}$.

Dark matter annihilation: In this model, the dark halo of the Milky Way is composed of particles which have a self-annihilation cross-section and number density sufficient to explain the required injected power. This scenario was first explored in the microwaves by Finkbeiner (2004b) and Hooper et al. (2007) and then expanded to include local cosmic-ray measurements by Cholis et al. (2009b). Recently, Dobler et al. (2011) showed that the gamma-ray spectrum, amplitude, and morphology can also be reproduced with dark matter annihilation if the dark halo is prolate and diffusion occurs preferentially along ordered field lines in the GC. Here the one significant failing of this model is that it does not produce sharp edges as seen in the *Fermi* data (the microwave morphology can be completely dominated by the magnetic field geometry). Thus, if these sharp edges persist with future data, the dark matter annihilation only model will be disfavored.

Of course, it is important to bear in mind that there may be multiple mechanisms operating at once (e.g., a bubble blown by a jet and filled with electrons by dark matter annihilation or a GC wind). In fact, this may be the only way to reconcile the very unusual features seen in the WMAP and *Fermi* data, especially given the flat brightness profile of the haze/bubbles which is not

reproduced in any of the above models.

6. SUMMARY

I have presented a last look at the WMAP haze/bubbles from the WMAP 7-year data, prior to the *Planck* data release. The haze morphology and spectrum are similar to previous analyses with several important differences. The inclusion of a disk template in the regression analysis suggests that the haze profile is somewhat flatter with latitude than previously thought. Furthermore, the sensitivity with seven years of data does permit a study of the emission at high (southern) latitudes. Here I find that there is haze emission at latitudes $|b| > 28^\circ$ and that there is a relatively sharp fall off in intensity for $b < -35^\circ$, most likely indicating a rapid fall off in the magnetic field strength at ~ 6 kpc within the haze/bubbles itself. As previously reported, the spectrum of the WMAP haze is too soft to be free-free emission and too hard to be generated by SN shocks (the “normal” particle acceleration mechanism) given diffusion effects. The spectrum is consistent with that required to produce the *Fermi* gamma-ray haze/bubbles, though I have illustrated that the two emissions at high latitudes are likely coming from mostly distinct parts of the cosmic-ray spectrum. While the haze is not strongly seen in the 7-year WMAP polarization data, I have shown that, even if the haze were not depolarized by turbulence in the magnetic field, the noise in the WMAP polarization data is sufficient to render a hard spectrum polarized component undetectable by comparison of K-band and Ka-band.

Lastly, everything that we have discovered to date about the haze/bubbles (hard spectrum synchrotron and gammas, sharp edges in the gammas, ± 10 kpc extent of the electrons, microwaves confined to lower latitudes, uniform intensity in gammas, lack of strong associated $H\alpha$ and strong polarization, low energy cutoff in electron spectrum, etc.) has made pinpointing a single underlying origin for the electron population very difficult. All of the proposed mechanisms have associated problems and if all of the haze/bubbles characteristics persist with future data, hybrid formation scenarios will likely be required.

Acknowledgments: I thank Tracy Slatyer, Ilias Cholis, Neal Weiner, Fulai Guo, Peng Oh, Doug Finkbeiner, and Igor Moskalenko for useful conversations. This work has been supported by the Harvey L. Karp Discovery Award.

REFERENCES

- Bennett, C. L., Hill, R. S., Hinshaw, G., et al. 2003a, *ApJS*, 148, 97
 Bennett, C. L., Halpern, M., Hinshaw, G., et al. 2003b, *ApJS*, 148, 1
 Biermann, P. L., Becker, J. K., Caceres, G., et al. 2010, *ApJ*, 710, L53
 Cholis, I., Dobler, G., Finkbeiner, D. P., et al. 2009a, *arXiv:0907.3953*
 Cholis, I., Dobler, G., Finkbeiner, D. P., Goodenough, L., & Weiner, N. 2009b, *Phys. Rev. D*, 80, 123518
 Crocker, R. M., & Aharonian, F. 2011, *Physical Review Letters*, 106, 101102
 Crocker, R. M., Jones, D. I., Aharonian, F., et al. 2011, *MNRAS*, 411, L11
 Dobler, G., Cholis, I., & Weiner, N. 2011, *ApJ*, 741, 25
 Dobler, G., Draine, B., & Finkbeiner, D. P. 2009, *ApJ*, 699, 1374
 Dobler, G., & Finkbeiner, D. P. 2008a, *ApJ*, 680, 1222
 —. 2008b, *ApJ*, 680, 1235
 Dobler, G., Finkbeiner, D. P., Cholis, I., Slatyer, T., & Weiner, N. 2010, *ApJ*, 717, 825
 Eriksen, H. K., Dickinson, C., Lawrence, C. R., et al. 2006, *ApJ*, 641, 665
 Finkbeiner, D. P. 2003, *ApJS*, 146, 407
 —. 2004a, *ApJ*, 614, 186
 —. 2004b, *arXiv:astro-ph/0409027*
 Finkbeiner, D. P., Davis, M., & Schlegel, D. J. 1999, *ApJ*, 524, 867
 Gold, B., Odegard, N., Weiland, J. L., et al. 2011, *ApJS*, 192, 15

- Guo, F., & Mathews, W. G. 2011, submitted to ApJ, arXiv:1103.0055
- Guo, F., Mathews, W. G., Dobler, G., & Oh, S. P. 2011, submitted to ApJ, arXiv:1110.0834
- Haslam, C. G. T., Salter, C. J., Stoffel, H., & Wilson, W. E. 1982, A&AS, 47, 1
- Hooper, D., Finkbeiner, D. P., & Dobler, G. 2007, Phys. Rev. D, 76, 083012
- Mertsch, P., & Sarkar, S. 2010, JCAP, 10, 19
- . 2011, Physical Review Letters, 107, 091101
- Miville-Deschênes, M.-A., Ysard, N., Lavabre, A., et al. 2008, A&A, 490, 1093
- Pietrobon, D., Gorski, K. M., Bartlett, J., et al. 2011, submitted to ApJ, arXiv:1110.5418
- Schlegel, D. J., Finkbeiner, D. P., & Davis, M. 1998, ApJ, 500, 525
- Schreier, E. J., Feigelson, E., Delvaille, J., et al. 1979, ApJ, 234, L39
- Spergel, D. N., Verde, L., Peiris, H. V., et al. 2003, ApJS, 148, 175
- Su, M., Slatyer, T. R., & Finkbeiner, D. P. 2010, ApJ, 724, 1044
- Veilleux, S., Cecil, G., & Bland-Hawthorn, J. 2005, ARA&A, 43, 769